Journal of
Ship&Ocean
Technology
©SEPTEMBER 2004

SOTECH Vol. 8, No. 3, pp. 26 ~ 39, 2004

Hull/Mooring/Riser Coupled Dynamic Analysis of a Turret–Moored FPSO Compared with OTRC Experiment

Young-Bok Kim[1] and Moo-Hyun Kim[2]

[1] Shipbuilding/Plant Research Institute, Samsung Heavy Industries, Gyeongnam, Korea;
E-mail: yb09.kim@samsung.com
[2] Civil Engineering Department, Texas A&M University, USA

Abstract

A vessel/mooring/riser coupled dynamic analysis program in time domain is developed for the global motion simulation of a turret-moored, tanker based FPSO designed for 6000-ft water depth. The vessel global motions and mooring tension are simulated for the non-parallel wind-wave-current 100-year hurricane condition in the Gulf of Mexico. The wind and current forces and moments are estimated from the OCIMF empirical data base for the given loading condition.

The numerical results are compared with the OTRC(Offshore Technology Research Center: Model Basin for Offshore Platforms in Texas A&M University) 1:60 model-testing results with truncated mooring system. The system's stiffness and line tension as well as natural periods and damping obtained from the OTRC measurement are checked through numerically simulated static-offset and free-decay tests. The global vessel motion simulations in the hurricane condition were conducted by varying lateral and longitudinal hull drag coefficients, different mooring and riser set up, and wind-exposed areas to better understand the sensitivity of the FPSO responses against empirical parameters. It is particularly stressed that the dynamic mooring tension can be greatly underestimated when truncated mooring system is used.

Keywords: vessel-mooring-riser coupled dynamics, turret-moored FPSO, truncated mooring, OTRC experiment, GoM non-parallel environmental condition

1 Introduction

FPSOs have been successfully installed and operated around the world during the past decade and many new FPSOs will be designed and installed in the coming years. In particular, with increasing interest in their use in the Gulf of Mexico, model tests were conducted at the Offshore Technology Research Center (OTRC) multi-directional wave basin to examine the behavior of generic FPSOs in wave, wind, and current conditions typical of the passage of severe hurricane (Ward et al 2001). FPSOs for the Gulf of Mexico will likely be passively moored through a turret system so that the tanker can weathervane or rotate in response to the changing wave, wind, and current directions in a hurricane. The waves, winds, and currents can be quite non-parallel, and subject the vessel

to quartering or beam seas that can significantly influence the response of a ship-shaped vessel.

In this study, a tanker-based turret-moored FPSO designed for the water depth of 6,000 ft and tested in the OTRC wave basin is adopted for the verification of the hull/mooring/riser coupled static and dynamic analyses by a computer program WINPOST-FPSO developed at Texas A&M University. The FPSO hull is moored by 12 chain-polyester-chain taut mooring system and also supports 13 steel catenary risers. A series of model tests were conducted at OTRC with statically-equivalent truncated mooring system. However in the model test, SCRs were not included. Since the water depth is large, it is expected in case of prototype that a significant portion of the total system damping comes from the long slender members and they may also contribute appreciably to the system's total stiffness and inertia. For the reasonable prediction of those static and dynamic quantities of the integrated system, the hull/mooring/riser coupled dynamic analysis is essential.

The present FPSO hull and mooring/riser system are very similar to those of full-loaded 6000ft-FPSO used in the DEEPSTAR study (Kim and Kim 2002). The major differences are turret location and vessel draft i.e. the vessel draft is changed from 18.9m to 15.12 m corresponding to 80 % of full-load draft and the turret position is 38.73-m (12.5% of Lpp) aft of the forward perpendicular of the vessel. The GoM 100-year non-parallel hurricane environmental conditions used in the OTRC model testing are also very similar to those of DEEPSTAR study. A scale of 1:60 was used in the OTRC model tests. Due to the limitation of basin depth, a truncated mooring system that can give reasonable surge stiffness was devised and used in the model testing. However, a separate numerical coupled dynamic analysis was conducted with the prototype mooring system extended to full water depth to indirectly observe the coupling effects and the problems and deficiency associated with the truncated mooring system.

In the present numerical analysis, the wind and current forces on the FPSO hull are generated from the OCIMF empirical data base developed for generic tankers. In the OCIMF data, only two sets of drag coefficients for the full and ballast loading conditions are given. Therefore, the wind/current force coefficients for the present 80% loading condition are linearly interpolated from the two sets of curves. The biggest uncertainty related to the reliability of FPSO global motion prediction lies on whether the empirical OCIMF data sets and the hull viscous damping coefficients from MARIN are sufficiently reliable or not. The wave loads and second-order drift forces are calculated by using the second-order diffraction/radiation 3D panel program WAMIT.

2 OTRC experimental results and design premise data

Here, the OTRC experimental results are compared with the simulation results by WINPOST-FPSO. The details of OTRC experiments were published in Ward et al (2001). The methodology of WINPOST-FPSO was published, for example, in Kim and Kim (2001). The paper contains the simulation results of the static offset test, the free-decay test, and hurricane-condition simulations for a 6000-ft FPSO adopted for DEEPSTAR study. In the OTRC experiments, the same FPSO hull shape and mooring system were used compared to the DEEPSTAR study but the turret location, vessel draft, and wind/current are different. Due to the change of vessel draft, loading condition, and turret position, many design parameters should be changed.

The top tension of the mooring lines is assumed to be the same as that of the DEEPSTAR FPSO. On the basis of this starting point, the weight balance is checked. The

displacement can be evaluated with the different loading condition data and corresponding draft. In the present 80% loading condition, the draft is given as 15.12 meters. The corresponding vessel displacement is calculated to be 187,060 MT. The details of the design premise data are shown in Table 1. The general arrangement and body plan of the vessel are shown in Figure 1. As shown in the above Figure, the vessel bow is toward the East (the bow is heading the East).

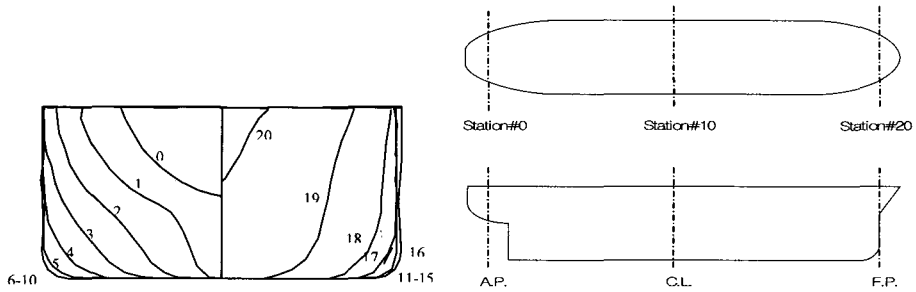

Figure 1: General arrangement and body plan of FPSO 6,000 ft.

Table 1: Main particulars of the turret moored for the OTRC FPSO

Description	Symbol	Unit	Quantity
Production level		*bpd*	120,000
Storage		*bbls*	1,440,000
Vessel size	kDWT	*m*	200
Length between perpendicular	Lpp	*m*	310.0
Breath	B	*m*	47.17
Depth	H	*m*	28.04
Draft (in full load)	T	*m*	15.121
Displacement (in full load)		*MT*	240,869
Length-beam ratio	L/B		6.57
Beam-draft ratio	B/T		3.12
Block coefficient	Cb		0.85
Center of buoyancy forward section 10	FB	*m*	6.6
Water plane area	A	m^2	12.878
Water plane coefficient	Cw		0.9164
Center of water plane area forward section 10	FA	*m*	1.0
Center of gravity above keel	KG	*m*	13.32
Transverse metacentric height	MGt	*m*	5.78
Longitudinal metacentric height	MGl	*m*	403.83
Roll raius of gyration in air	R_{xx}	*m*	-
Pitch raius of gyration in air	R_{yy}	*m*	-
Yaw raius of gyration in air	R_{zz}	*m*	-
Frontal wind area	Af	m^2	-
Transverse wind area	Ab	m^2	-
Turret in center line behind Fpp (12.5 % Lpp)	Xtur	*m*	38.73
Turret elevation below tanker base	Ztur	*m*	1.52
Turret diameter		*m*	15.85

Table 2: Main particulars of mooring systems for the OTRC FPSO

Designation	Unit	Quantity
Water depth	*m*	1829
Pre-tension	*kN*	1424
Number of lines		4×3
Degree between the 3 lines	*deg.*	5
Length of mooring line	*m*	2652
Radius of location of chain stoppers on turn table	*m*	7.0
Segment 1(ground section): Chain		
Length at anchor point	*m*	121.9
Diameter	*Cm*	9.52
Dry weight	*N/m*	1856
Weight in water	*N/m*	1615
Stiffness AE	*kN*	912120
Mean breaking load (MBL)	*kN*	7553
Segment 2: wire (Polyester)		
Length	*m*	2438
Diameter	*Cm*	16.0
Dry weight	*N/m*	168.7
Weight in water	*N/m*	44.1
Stiffness AE	*kN*	186800
Mean breaking load (MBL)	*kN*	7429
Segment 1(ground section): Chain		
Length at anchor point	*m*	91.4
Diameter	*Cm*	9.53
Dry weight	*N/m*	1856
Weight in water	*N/m*	1615
Stiffness AE	*kN*	912120
Mean breaking load (MBL)	*kN*	7553

The mooring lines and risers are hinged to and spread from the turret. In the original design data there are 12 combined mooring lines consisting of chain, polyester, and chain, and 13 steel catenary risers. There are 4 groups of mooring lines, each group consists of 3 mooring lines 5-degrees apart. The center of the first group is heading the true East, and so the second group is toward the true North etc. Each mooring line has a studless chain anchor of Grade K4. Table 2 shows the main particulars of original target mooring lines. Table 3 gives the hydrodynamic coefficients for mooring lines. In the present analysis, the effects of tangential drag and added inertia of mooring lines and Coulomb friction from seabed are expected to be unimportant, and thus they are not included in the analysis.

Table 3: Hydrodynamic coefficients of the chain, rope and wire for the OTRC FPSO

Hydrodynamic Coefficients	Symbol	Chain	Rope/Poly
Normal drag	C_{dn}	2.45	1.2
Tangential drag	C_{dt}	0.65	0.3
normal added inertia coefficient	C_{in}	2.00	1.15
Tangential added inertia coefficient	C_{it}	0.50	0.2
Coulomb friction over seabed	F	1.00	0.6

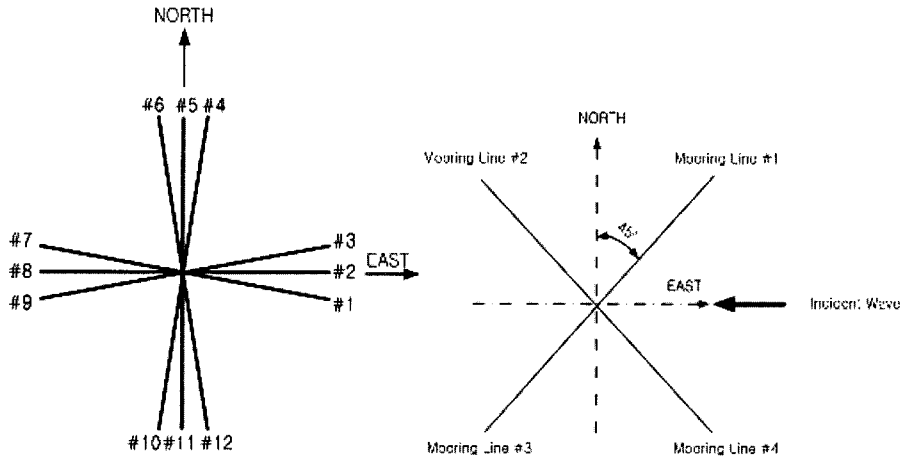

(a) (b)

Figure 2: Arrangement of mooring lines for turret-moored FPSO:
(a) Mooring system of the original FPSO
(b) Mooring system of the OTRC experiment

In the OTRC model testing, the mooring design and arrangement are modified i.e. only four equivalent mooring lines were used in X shape without risers. One equivalent mooring line represents the combined effects of 3 mooring lines. Figure 2 shows the difference between original and equivalent mooring arrangement. The equivalent mooring lines are in X shape and spread 90 degrees apart from the adjacent mooring lines. The #1 equivalent mooring has 45-degree orientation from the true East etc. With respect to the x- and y-axis (the x-axis toward the East and the y-axis toward the North), the mooring lines are arranged symmetrically.

In the numerical model for this study, the full-length X-shaped prototype mooring system is devised so that their surge stiffness and the total drag force are as close as possible to the original target mooring system. However, the truncated mooring system devised in the experiment to represent the same target original mooring system is not numerically modeled because it contains springs, clump weights, and buoys which make the numerical modeling more difficult. The total length of the truncated mooring used in the experiment was 43ft (2580 ft in full scale), while the actual length in full scale is 8700ft.

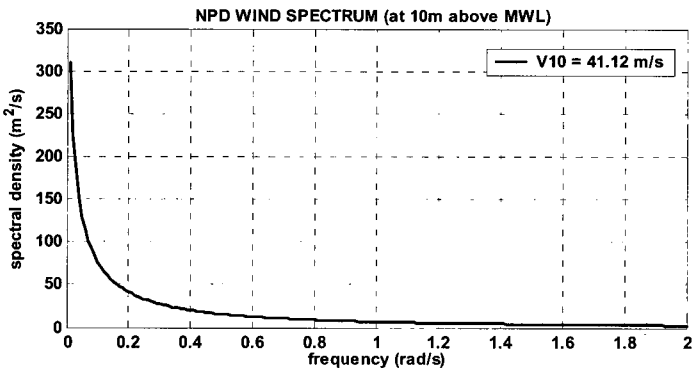

Figure 3: NPD wind spectrum (at 10 m above MWL, V10 = 41.12).

3 Environmental data

For experiments and simulations, the following 100-year extreme hurricane condition at the Gulf of Mexico (GoM) is used as the DeepStar case. The wave condition is given by JONSWAP spectrum with significant wave height of 12 m, the peak period of 14 sec, and the overshooting parameter of 2.5. To generate wind loading, the NPD wind spectrum was used, which is shown in Figure 3. In the DeepStar study, the API wind spectrum with the same input parameters was used. The mean wind velocity at the reference height of 10 m for one hour is 41.12 m/s.

The current is mainly induced by the storm. The current velocity near free surface is 0.91m/s. The wind and current directions are swapped compared to DeepStar study.

For the intermediate region between 60.96 m to 91.44 m, the current profile is varied linearly. In numerical simulations, the current is assumed to be steady and uni-directional. The summary of the environmental conditions for this study is shown in Table 4.

Table 4: Environmental loading condition for the OTRC FPSO

Description	Unit	Quantity
Wave		
Significant wave height, Hs	m	12.19
Peak period, Tp	sec	14
Wave spectrum	*JONSWAP (γ =2.5)*	
Direction	deg	180[1)]
Wind		
Velocity	m/s	41.12m/s @10m
Spectrum	*API RP 2A-WSD*	
Direction	deg	150[1)]
Current		
Profile		
at free surface (0 m)	m/s	0.9144
at 60.96 m	m/s	0.9144
at 91.44 m	m/s	0.0914
on the sea bottom	m/s	0.0914
Direction	deg	210[1)]

Remark: [1)] The angle is measured counterclockwise from the x-axis (the East)

4 Numerical modeling

The design data $L \times B \times D$, T, KG, the turret position, and the top tension of mooring lines etc. are taken from Ward et al(2001). In the same paper, natural frequencies and damping measured from the free decay test in the OTRC wave basin are also given. The added mass and radiation damping, first-order wave-frequency forces, and second-order mean and difference-frequency forces are calculated from the 3D second-order

diffraction/radiation panel program WAMIT. Figure 4 shows the distribution of pan the body surface. Taking advantage of symmetry, only half domain is discretized (panels for hull and 480 panels for free surface). All the hydrodynamic coefficients \ calculated in the frequency domain, and then the corresponding forces were convertec the time domain using two-term Volterra series expansion. The frequency-depende radiation damping was included in the form of convolution integral in the time doma equation. The wave drift damping was expected to be small and thus not included in the ensuing analysis.

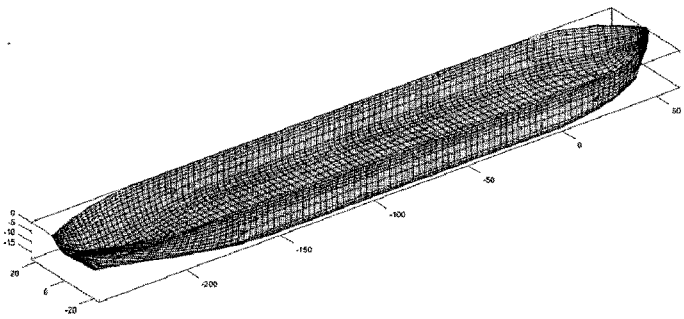

Figure 4: Mesh generation of the turret-moored FPSO.

The methodology for hull/mooring/riser coupled statics/dynamics is similar to that of Kim and Kim(2002). The mooring lines are assumed hinged at the turret and anchor position. The wave force quadratic transfer functions are computed for 9 wave frequencies, ranging from 0.24 to 1.8 rad/sec and the intermediate values for other frequencies are interpolated. The hydrodynamic coefficients and wave forces are expected to vary appreciably with large yaw angles and the effects should be taken into consideration for the reliable prediction of FPSO global motions. Therefore, they are calculated in advance for various yaw angles with 5-degree interval and the data are then tabulated as inputs.

The second-order diffraction/radiation computation for a 3D body is computationally very intensive especially when it has to be run for various yaw angles. Therefore, many researchers avoided such a complex procedure and have instead used simpler approach called Newman's approximation i.e. the off-diagonal components of the second-order difference-frequency QTFs are approximated by their diagonal values (mean drift forces and moments). The approximation can be justified when the relevant natural frequency is very small and the slope of QTFs near the diagonal is not large. In Kim and Kim(2002) the validity of Newman's approximation is tested to be reasonable against more accurate results with complete QTFs.

From the WAMIT output, the displacement volume, the center of buoyancy and the restoring coefficients can be obtained. The obtained data from the WAMIT output is summarized in Table 5. Based on these data, the vertical static equilibrium of the FPSO an be checked i.e. the sum of the vertical line top tensions and the weight is to be equal to e buoyancy. The relations between the natural frequency, and the restoring coefficients t the masses are defined as follows:

$$f = \frac{1}{2\pi}\sqrt{\frac{C_{ij}}{M_{Vij}}} \quad \text{(1/sec or Hz)} \qquad (i,j = 1,2,\cdots,6) \tag{1}$$

where f is the natural frequency, C_{ij} is the restoring coefficients (hydrostatic + mooring) in which i and j can be any combination of six DOF, and $M_{Vij}(=M_{aij}+M_{ij})$ is the virtual mass in which M_{aij} is the added mass near natural frequencies and m_{ij} is the mass of the body in the i and j direction. The relationship between m_{ij} and W are as follows:

$$m_{33} = W \tag{2}$$

$$m_{44} = W(R_{xx}^2 + z_g^2 + y_g^2) \tag{3}$$

$$m_{55} = W(R_{yy}^2 + z_g^2 + x_g^2) \tag{4}$$

where (x_g, y_g, z_g) is the coordinate of center of the gravity, and R_{xx}, R_{yy} are the radii of gyrations for roll and pitch motions with respect to the center of gravity. From the WAMIT output, M_{Vij} can be obtained. These data are also summarized in Table 5.

Table 5: WAMIT output and vessel data

Description	Symbol	Unit	Quantity	Reference
Displaced volumn	$\forall$	m^3	182,499	WAMIT
Buoyancy	B	m.ton	187,060	$\forall \times \rho_w$
Total top tension	T	kN	11,649	Given data
Weight in mass	W	m.ton	185,870	Static equilibrium
Center of gravity	x_g	m	-109.670	Given data
	z_g	m	-1.801	
Center of buoyancy	x_b	m	-89.086	WAMIT
	z_b	m	-7.401	
Restoring coefficients	$\overline{C_{33}}$		56.3226	WAMIT
	$\overline{C_{33}}$		22.3251	
	$\overline{C_{33}}$		4688.27	
Added mass/moment	M_{a33}	m.ton	1.9566E+05	WAMIT
	M_{a44}	m.ton-m^2	1.1018E+07	
	M_{a55}	m.ton-m^2	3.5189E+09	

The restoring coefficients are defined by:

$$C_{33} = \rho_w g A_w, \qquad \overline{C_{33}} = \frac{C_{33}}{\rho_w g L_R^2} \tag{5}$$

$$C_{44} = \rho_w g \iint_{A_W} y^2 n_3 ds + \rho_w g \forall z_b - mgz_g, \qquad \overline{C_{44}} = \frac{C_{44}}{\rho_w g L_R^4} \tag{6}$$

$$C_{55} = \rho_w g \iint_{A_W} x^2 n_3 ds + \rho_w g \forall z_b - mgz_g, \qquad \overline{C_{55}} = \frac{C_{55}}{\rho_w g L_R^4} \tag{7}$$

where $\overline{C_{33}}$, $\overline{C_{44}}$ and $\overline{C_{55}}$ are the non-dimensionalized restoring coefficients, ρ_w and A_w are the water density and the water plane area, $\forall$ is the displaced volume, Z_b is the z-coordinate of the center of buoyancy, $m(=W)$ is the mass of the body and L_R is the reference length (vessel draft), and n_3 represents the directional cosine in z-direction. Therefore, if the data in Table 6 and the equation (2) to (7) are used, the radii of gyrations and restoring coefficients can be estimated. The acquired data are summarized in Table 6.

Table 6: Re-estimated data from WAMIT output.

Description	Symbol	Unit	Quantity
Water plane area	Aw	m^2	12,878
Radius of roll gyration	R_{xx}	m	14.04
Radius of pitch gyration	R_{yy}	m	79.67
Radius of yaw gyration	R_{zz}	m	81.4

5 Results and discussion

5.1 Static offset test with re-generated model data

The static offset tests are performed by WINPOST-FPSO with the numerical model established as described in the previous section. The test results are plotted in Figure 5. They show that the stiffness of the numerical model with original full riser/mooring system is in good agreement with the target stiffness of OTRC model testing provided by Marin. The present full scale numerical model with X-shaped mooring system gives almost the same surge stiffness compared to the target but there exist nontrivial difference in the tension of individual mooring line although the overall trend is very similar. The truncated mooring system designed for OTRC experiment is almost linear and only approximately follows the target value.

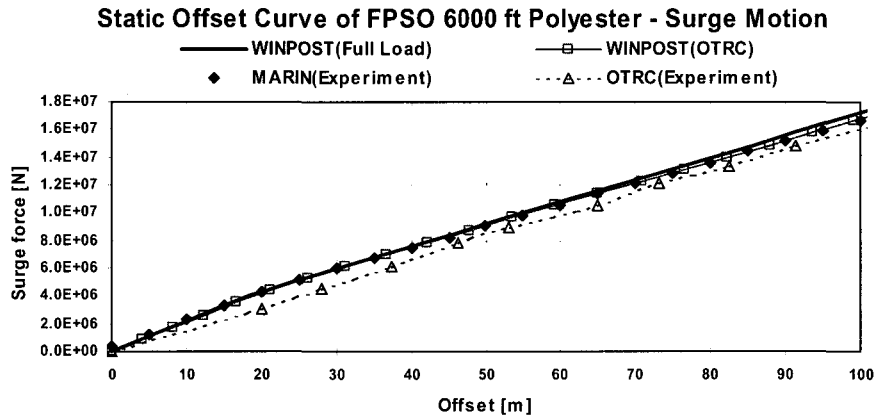

(a)Static offset curves for surge motion obtained by experiments and WINPOST-FPSO

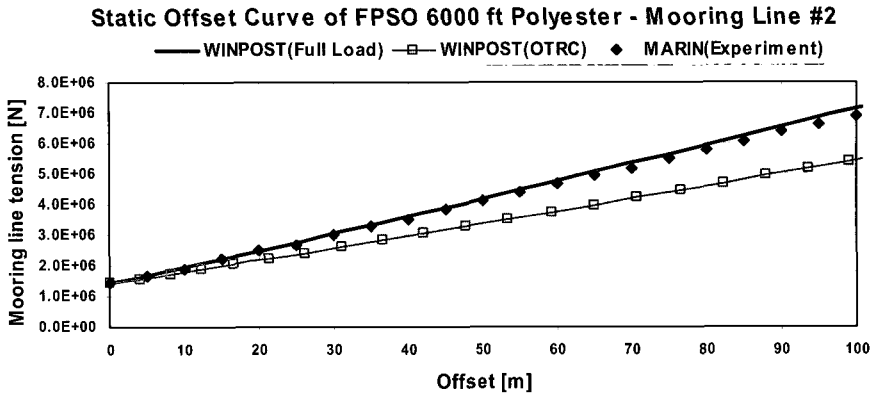

(b) Static offset test result of #2 mooring line in the surge direction

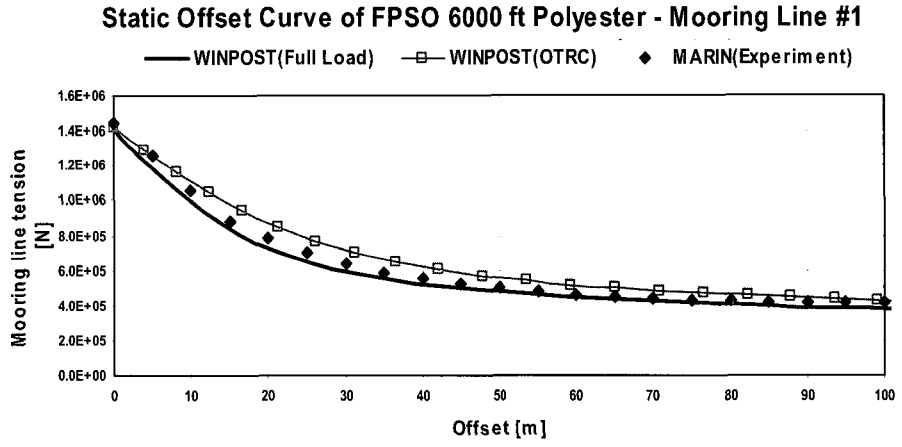

(c) Static offset test result of #1 mooring line in the surge direction

Figure 5: Comparison of the static offset test results.

5.2 Free decay test with re-generated model data

The total damping of the hull/mooring system can be obtained from the free decay tests and the numerical results are compared with the OTRC experiments. The last column (4 equivalent mooring lines without riser) corresponds to the OTRC experiment. From the free-decay time histories, the natural period and damping of the system can be read. First, the comparisons of natural periods for various modes look satisfactory ensuring the proper numerical modeling of the real system. It can also be seen that the riser tension contributes appreciably to the heave and pitch natural periods. Second, there exist some discrepancies in the predicted and measured values of damping ratios. The difference in roll damping is particularly noticeable because of the viscous effect. The experimental damping value in the parenthesis is without considering added mass effect in normalization. The damping in general depends on motion amplitudes i.e. damping is larger in greater motion amplitudes.

The truncated mooring system with clumps and buoys cannot very well represent the prototype full-length mooring system (Kim 1993, Ran and Kim 1997).

5.3 Time simulation results for 100-yr nonparallel hurricane

The comparison of the OTRC experiment and the WINPOST-FPSO simulation is shown in Table 8. In the table, two types of hull drag coefficients proposed by Wichers (1988, 2001) are used as shown in Figure 6. The first one is for calm water and the second one in the presence of current. The first column in the table is for the hull drag coefficients without considering the current. In the second and third columns of the table, the hull drag coefficients considering the current are used. When the current effects are considered, the analysis results follow the experimental results better in sway and roll, but in surge and yaw motion, there are still rather big differences between them. The differences can be attributed to many possible mismatches between numerical and physical models, such as truncated mooring system, wind and current generation, etc. In the first 3 columns of numerical results, the frontal and lateral wind areas are increased by 20 % and 30 % considering the increased hull wind-exposed area compared to the full load case. In the last column, however, the original wind area was used. The difference in the projected wind areas can result in the differences in yaw angle and slowly varying motions.

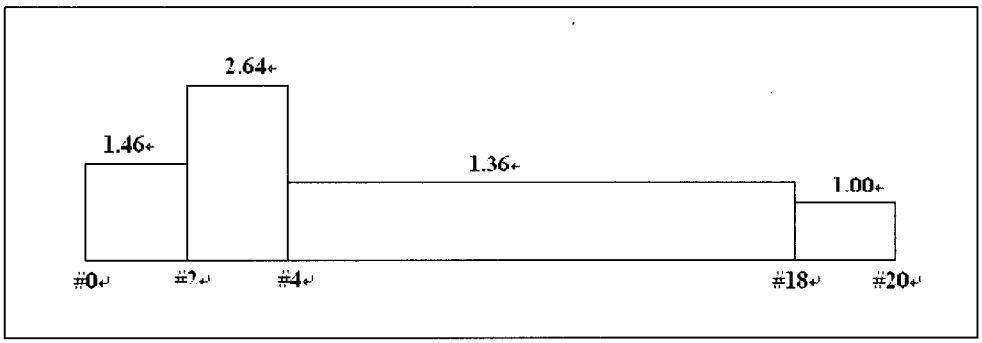

(a) Hull drag coefficients not in consideration of the current effect

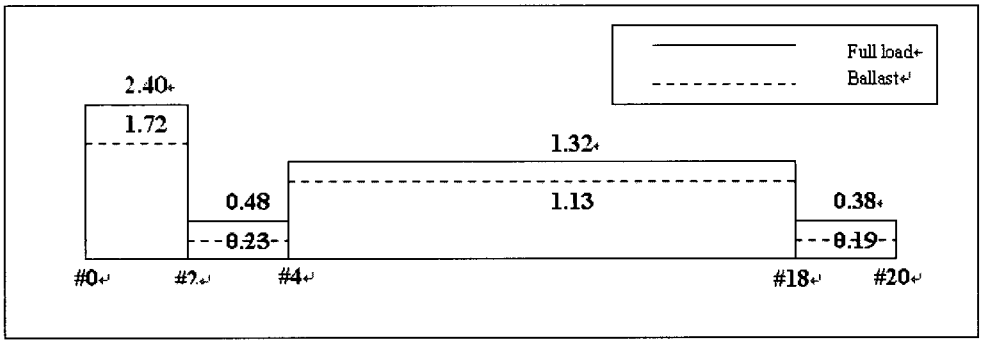

(b) Hull drag coefficients in consideration of the current effect

Figure 6: Hull drag coefficients proposed by Wichers (1988 and 2001)

The differences in dynamic mooring tension are very conspicuous i.e. measured dynamic tension is greatly smaller than the predicted one. They are mainly caused by the mooring line truncation in the experiment due to the depth limitation of the OTRC wave

basin (Kim 1993, Ran and Kim 1997). The surge stiffness was matched in the model testing by using clumps/buoys and springs. However, it may give different stiffness and/or dynamic characteristics in other modes. In the last column, the drag coefficients in surge are multiplied by 2.5 (original longitudinal Cd=1.0) to observe the drag force effect in surge.

Table 7: Comparison of the free decay test results.

	OTRC Experiment (4 eqiv. Mooring Lines)		WINPOST					
			12 mooring lines +13 risers		4 equiv. moorings +1 riser		4 equiv. mooring lines w/o riser	
	period (sec)	damping (%)	period (sec)	damping (%)	period (sec)	damping (%)	period (sec)	damping (%)
surge (m)	206.8	3.0 (3.0)	182.5	5.8	181.5	5.5	193.8	4.9
heave (m)	10.7	6.7 (13.9)	8.2	6.0	10.4	5.1	10.9	5.1
roll (deg)	12.7	3.4 (4.4)	13.4	0.9	12.7	1.1	12.6	0.8
pitch (deg)	10.5	8 (16.5)	13.9	6.0	10.8	8.5	10.9	8.5

Table 8: Comparison of time simulation results

		OTRC Experiment	WINPOST (with 4-equiv. line model)			
			Old Sway Cd (1.5hrs)	New Sway Cd (1.5hrs)	New Sway Cd and Surge Cd (1.5hrs)	New Sway and Surge Cd*2.5+old wind area (3hrs)
Motion						
surge (m)	mean	-22.92	-25.22	-20.26	-19.39	-20.89
	min.	-61.26	-83.10	-83.33	-78.64	-88.72
	max.	2.29	21.31	22.67	18.94	24.49
	rms.	9.72	24.13	23.18	21.02	18.84
sway (m)	mean	-0.09	4.76	2.99	2.90	3.66
	min.	-21.43	-8.17	-8.21	-7.15	-12.14
	max.	13.08	22.96	21.67	21.18	31.75
	rms.	4.57	6.48	5.44	5.16	5.96
roll (deg)	mean	-0.10	-0.72	-0.59	-0.54	-0.38
	min.	-3.60	-11.41	-11.91	-11.70	-14.95
	max.	3.50	8.89	9.20	8.47	9.58
	rms.	0.90	3.52	3.73	3.27	3.68
yaw (deg)	mean	-16.00	-10.25	-14.81	-16.16	-11.02
	min.	-24.60	-20.23	-22.95	-22.61	-24.07
	max.	-3.40	-1.49	-6.67	-7.79	5.55
	rms.	3.80	4.18	3.11	2.84	5.48
Mooring tension						
Mooring line #1 (kN)	mean	5,907	6,403	6,487	6,440	7,757
	min.	3,679	1,230	1,218	1,566	2,447
	max.	10,360	14,600	14,893	14,173	16,783
	rms.	827	2,688	2,735	2,565	2,359
Mooring line #2 (kN)	mean		2,400	2,379	2,333	3,457
	min.		197	202	204	511
	max.		7,883	7,853	7,537	9,537
	rms.		2,046	2,036	1,931	1,506
Mooring line #3 (kN)	mean		2,644	2,593	2,562	3,657
	min.		630	530	782	1,163
	max.		7,540	7,543	7,067	9,233
	rms.		1,893	1,898	1,796	1,346
Mooring line #4 (kN)	mean	5,600	7,597	7,643	7,590	8,803
	min.	2,927	802	827	1,041	2,511
	max.	8,127	13,333	13,600	12,800	23,697
	rms.	801	2,020	2,047	1,870	3,560

The measured mean line tension is less than the predicted one mainly because of the discrepancy in static offset curve. As for global vessel motions, the analysis results are reasonable compared to the experiments in view of overall trend. It needs to be reminded one more time that in the present simulations, the Newman's approximation scheme is used for evaluating the second-order difference-frequency wave forces and wave drift damping neglected.

6 Summary and conclusions

In the present study, the global motions and mooring dynamics of a deepwater turret-moored FPSO in non-parallel 100-yr hurricane are numerically simulated and the numerical results are compared with the OTRC 1:60 model-testing results with truncated mooring system. The system's stiffness and line tension as well as natural periods obtained from the OTRC measurement are checked through numerically simulated static-offset and free-decay tests by WINPOST.

In particular, the free-decay tests were repeated for different mooring/riser combination to observe the contributions of mooring lines and risers. The global vessel motion simulations in the hurricane condition were conducted by varying lateral and longitudinal hull drag coefficients and wind-exposed areas to better understand the sensitivity of the FPSO against empirical parameters. The differences between measured and predicted results can be attributed to the wind force generation, the current profile control, the mooring line truncation, and the usage of springs/buoys/clumps in truncated mooring lines. It is particularly stressed that the dynamic mooring tension can be greatly underestimated when truncated mooring system is used.

References

Arcandra, T. 2001. Hull/Mooring/Riser Coupled Dynamic Analysis of a Deepwater Floating Platform with Polyester Lines. Ph.D. Dissertation, Texas A&M University.

Arcandra, T., P. Nurtjahyo and M.H. Kim. 2002. Hull/mooring/riser coupled analysis of a turret-moored FPSO 6000 ft: comparison between polyester and buoys-steel mooring lines. Proc. 11th Offshore Symposium, The Texas Section of the Society of Naval Architects and Marine Engineers, SNAME, 1-8.

Baar, J.J.M, C.N. Heyl and G. Rodenbusch. 2000. Extreme responses of turret moored tankers. Proc. Offshore Technology Conference, OTC 12147 [CD-ROM], Houston, Texas.

Dean, R.G. and R.A. Dalrymple. 1992. Water Wave Mechanics for Engineers and Scientists. Advanced Series on Ocean Engineering, **2**. World Scientific Press, Dover, D.E.

Faltinsen, O.M. 1998. Sea Loads on Ships and Offshore Structures. The Cambridge University Press, Cambridge.

Garrett, D.L. 1982. Dynamic analysis of slender rods. J. Energy Resources Technology, Trans. of ASME, **104**, 302-307.

Kim, M.H. 1992. WINPOST V3.0 Users Manual. Dept. of Ocean Engineering, Texas A&M University.

Kim, M.H, R.S. Mercier, G. Gu, C. Wu and D. Botelho. 1993. PC-based wave load computation for large volume multi_column structures. Proc. of the 4th Int. Offshore and Polar Eng. Conference, ISOPE.

Kim, M.H., T. Arcandra and Y.B. Kim. 2001a. Validability of spar motion analysis against various design methodologies/parameters. Proc. 20th Offshore Mechanics and Arctic Eng. Conference, OMAE01-OFT1063 [CD-ROM], L.A., Califonia.

Kim, M.H., T. Arcandra and Y.B. Kim. 2001b. Validability of TLP motion analysis against various design methodologies/parameters. Proc. 12th Int. Offshore and Polar Eng. Conference, ISOPE, **3**, 465-473.

Kim, M.H. and Y.B. Kim. 2002. Hull/mooring/riser coupled dynamic analysis of a tanker-based turret-moored FPSO in deep water. Proc. 13th Int. Offshore and Polar Eng. Conference, ISOPE .

Lee, C.H. 1999. WAMIT User Manual. Dept. of Ocean Engineering, Massachusetts Institute of Technology, Cambridge, M.A.

Ma, W., M.Y. Lee, J. Zou and E. Huang. 2000. Deep water nonlinear coupled analysis tool. Proc. Offshore Technology Conference, OTC 12085 [CD-ROM], Houston, Texas.

Nordgen, R.P. 1974. On computation of the motions of elastic rods. ASME J. Applied Mechanics, 777-780.

OCIMF 1994 Prediction of Wind and Current Loads on VLCCs. 2nd Edition, Witherby & Co. Ltd, London, England.

Ran, Z. and M.H. Kim. 1997. Nonlinear coupled responses of a tethered spar platform in waves. Proc. of the 8th Int. Offshore and Polar Eng. Conference, ISOPE.

Ward, E.G., M.B. Irani and R.P. Johnson. 2001. The behavior of a tanker-based FPSO in hurricane waves, Winds, and Currents. Proc. 11th Int. Offshore and Polar Eng. Conference, ISOPE, **4**, 650-653.

Wichers, J.E.W. 1988. A Simulation Model for a Single Point Moored Tanker. Ph.D. Dissertation, Delft University of Technology, Delft, The Netherlands.

Wichers, J.E.W. and C. Ji. 2000a. On the coupling term in the low-frquency viscous reaction forces of moored tankers in deep water. Proc. Offshore Technology Conference, OTC 12086 [CD-ROM], Houston, Texas.

Wichers, J.E.W and C. Ji. 2000b. Deepstar-CTR 4401- theme structure benchmark analysis for tanker based FPSO-GoM. Technical Rep. **15629-1-OE**, MARIN, Wageningen, The Netherlands.

Wichers, J.E.W. and P.V. Develin. 2001. Effect of coupling of mooring lines and risers on the design values for a turret moored FPSO in deep water of the gulf of mexico. Proc. 11th Int. Offshore and Polar Eng. Conference, ISOPE, **3**, 480-487.

Wichers, J.E.W, H.J. Voogt, H.W. Roelofs and P.C.M. Driessen. 2001. Deepstar-CTR 4401- benchmark model test. Technical Rep. **16417-1-OB**, MARIN, Wageningen, The Netherlands.